Available online at www.sciencedirect.com
SCIENCE DIRECT®
ELSEVIER
C. R. Physique 5 (2004) 769–780
COMPTES RENDUS PHYSIQUE
http://france.elsevier.com/direct/COMREN/
Ice: from dislocations to icy satellites/La glace : des dislocations aux satellites de glace

# Internal structure and dynamics of the large icy satellites

Christophe Sotin *, Gabriel Tobie

*Laboratoire de planétologie et géodynamique, UMR-CNRS 6112, faculté des sciences, 2, rue de la Houssinière, BP 92208, 44322 Nantes cedex 3, France*

Available online 6 October 2004

Presented by Guy Laval

**Abstract**

The magnetic data returned by the Galileo mission suggest that deep oceans are present within the icy Galilean satellites. In addition, tectonic features on Europa are consistent with models of subsolidus convection within the outer ice I layer. Ice viscosity is a key parameter for modeling the thermal and orbital evolution of these large satellites. Using laboratory experiments and glacier measurements, this article shows that tidal heating is a strong source of internal heating which may explain the presence of a deep ocean within Europa. Another key parameter is the composition of ice. The presence of ammonia, which is likely in Saturn's sub-nebula, decreases so much the melting point temperature of ice that it would inhibit the complete freezing of the ocean. Predictions for the internal structure of Titan are made and will be checked by the Cassini mission which started orbiting Saturn on 1st July 2004. ***To cite this article: C. Sotin, G. Tobie, C. R. Physique 5 (2004).***


**Résumé**

**Structure interne et dynamique des grands satellites de glace.** Les données magnétiques de la mission Galiléo sont compatibles avec l'existence d'un ocean à l'intérieur des grands satellites de glace de Jupiter. D'autre part, la tectonique d'Europe suggère l'existence de mouvements de convection dans la cryosphère de glace I. La viscosité de la glace est un paramètre clé pour modéliser l'évolution thermique et l'évolution orbitale de ces satellites. Grâce aux données de laboratoire et à celles obtenues sur les glaciers terrestres, ce papier montre que la dissipation de chaleur par effets de marée est si importante qu'elle permet d'expliquer la présence d'un océan à l'intérieur d'Europe. L'ammoniaque est un autre paramètre important car sa présence abaisse tellement la température de fusion des hydrates qu'un océan ne peut totalement cristalliser. Un modèle de structure interne est proposé pour Titan et cette prédiction sera confrontée aux données de la mission Cassini–Huygens qui est en orbite autour de Saturne depuis le 1 juillet 2004. ***Pour citer cet article : C. Sotin, G. Tobie, C. R. Physique 5 (2004).***


*Keywords:* Icy satellites; Galileo mission; Cassini–Huygens mission; Titan; Ice viscosity

*Mots-clés :* Satellites de glace ; Mission Galiléo ; Mission Cassini–Huygens ; Titan ; Viscosité des glaces

## 1. Introduction

Ice is a major component of the outer solar system bodies which formed beyond the snow line, which is the limit where ice can condensate. The large amount of ice enabled the rapid formation of big planetary embryos, more than 10 times the

* Corresponding author.
*E-mail address:* Christophe.Sotin@chimie.univ-nantes.fr (C. Sotin).

1631-0705/$ – see front matter © 2004 Académie des sciences. Published by Elsevier SAS. All rights reserved.
doi:10.1016/j.crhy.2004.08.001

Table 1
Characteristics of the largest icy satellites and Io. The first column gives the planet (J for Jupiter, S for Saturn, U for Uranus and N for Neptune). This table provides the data for the biggest icy satellites. To assess the radiogenic power at present time, we assume that the density of silicates is 3528 $kg/m^3$, a value equal to Io's density. Values of the MoI factor come from the compilation of Sohl et al. [24]. A MoI factor of 0.4 means that the satellite is not differentiated

| | | $\rho$ ($kg/m^3$) | Radius (km) | Mass ($10^{22}$ kg) | Eccen-tricity | Prot (days) | Mass of silicates ($10^{22}$ kg) | %mass of ice | Power (TW) | MoI factor |
|---|---|---|---|---|---|---|---|---|---|---|
| J | IO | 3528 | 1822 | 8.938 | 0.004 | 1.77 | 8.938 | 0 | 0.536 | 0.377 |
| | EUROPA | 2970 | 1569 | 4.805 | 0.010 | 3.55 | 4.448 | 7.4 | 0.267 | 0.346 |
| | GANYMEDE | 1940 | 2634 | 14.850 | 0.0015 | 7.15 | 10.042 | 32.4 | 0.603 | 0.311 |
| | CALLISTO | 1851 | 2403 | 10.759 | 0.007 | 16.70 | 6.903 | 35.8 | 0.414 | 0.355 |
| S | TITAN | 1881 | 2575 | 13.453 | 0.029 | 15.95 | 8.793 | 34.6 | 0.528 | ? |
| | RHEA | 1240 | 764 | 0.232 | 0.001 | 4.52 | 0.063 | 73 | 0.004 | ? |
| U | TITANIA | 1710 | 790 | 0.353 | 0.002 | 8.71 | 0.205 | 42.1 | 0.012 | ? |
| N | TRITON | 2054 | 1353 | 2.131 | 0 | R5.88 | 1.526 | 28.4 | 0.092 | ? |
| | PLUTON | 2050 | 1152 | 1.313 | | | 0.938 | 28.5 | 0.056 | ? |
| | CHARON | 2020 | 593 | 0.176 | $<0.001$ | 6.39 | 0.124 | 29.5 | 0.007 | ? |

Earth's mass, which were then able to retain light gazes such as $H_2$ and He, which are the main components of the giant planets (e.g., [1,2]). The formation of the giant planets was accompanied by the formation of icy satellites with different sizes and mass fraction of ice (Table 1) within their sub-nebula [3,4]. The Voyager exploration of the outer planets from the late seventies to late eighties revealed the diversity and the complexity of the different icy moons orbiting around the giant planet. Most of the icy bodies, from few hundred to five thousand kilometers in diameter, exhibit tectonic features, indicating past and maybe present surface activities. Two of the most striking discoveries were the intense silicate volcanism on Io [5] and the complex structure on Europa's surface [6,7]. Even small icy satellites like Mimas [8], a satellite of Uranus, or Enceladus [9], a satellite of Saturn, show endogenic surface features, witness for episodes of cryovolcanism and tectonism. The dense atmosphere of Titan and the geysers of Triton indicate the possibility of the degassing process [10,11], and that volatile molecules such as ammonia or methane are stored in their interior (e.g. [12]). The first detailed study of the Jovian icy satellites by a space mission, the NASA Galileo mission (1996–2003), has definitely proven that the icy bodies are complex worlds of great interest for exobiology and for understanding processes similar to those existing on Earth (tectonics, heat transfer, magnetism). From July 2004, the NASA-ESA Cassini–Huygens mission provides new data sets on Saturn's icy satellites, notably Titan, the largest moon coated by a dense methane rich atmosphere. The Huygens probe will penetrate this unique atmosphere in January 2005.

Models describing the formation of large satellites (e.g. [13]) predict that a large amount of the primordial ice melted during the accretion process, forming a liquid water layer in the outer part of the satellite, which then progressively crystallizes as the satellite interior cools down. Surface images and magnetic data collected during the last six years by the Galileo mission, suggest that a liquid layer is still present within Europa, Callisto and Ganymede [14–18]. The presence of an ocean within the icy satellites is surprising since one may expect these satellites to be frozen due to the very cold surface temperature (100 K) and their relatively small size. The crystallization rate depends on both the heat sources available within the satellite and heat transfer toward the surface, which is controlled by the properties of ice. Two processes mainly control the evolution of an icy satellite: (i) thermal convection in the ice layer, which is a very efficient cooling process; and (ii) tidal dissipation, which can provide a large heating rate. In both processes, ice rheology is a key parameter. There is continually a competition between the convective transfer and the heat generation in the outer ice Ih layer, which are coupled through the viscous properties of ice.

After describing our present knowledge of the internal structure of the large icy satellites, this article addresses the problem of their internal dynamics. The predictions from these models depend strongly on the viscous law which is used for describing the creep behavior of ice, and on the presence of salts and/or volatiles such as ammonia that modify the physical properties of ice. These effects are discussed in the last part of the article.

## 2. Internal structure

Interior models can be constrained from geophysical data. The interior models are one-dimensional because lateral variations are considered to have second order effect. Additional constraints are obtained by incorporating equations of state (EoS) of the different materials which compose the satellite. These EoS link the density ($\rho$) to pressure ($P$) and temperature ($T$). Hydrostatic equilibrium ($\mathrm{d}P/\mathrm{d}r = -\rho g$ where $g$ is gravity acceleration) provides the additional equation to get the pressure profile. Heat transfer models provide the temperature profile (see Section 2). Since an icy satellites may contain ice, silicates and iron alloys,

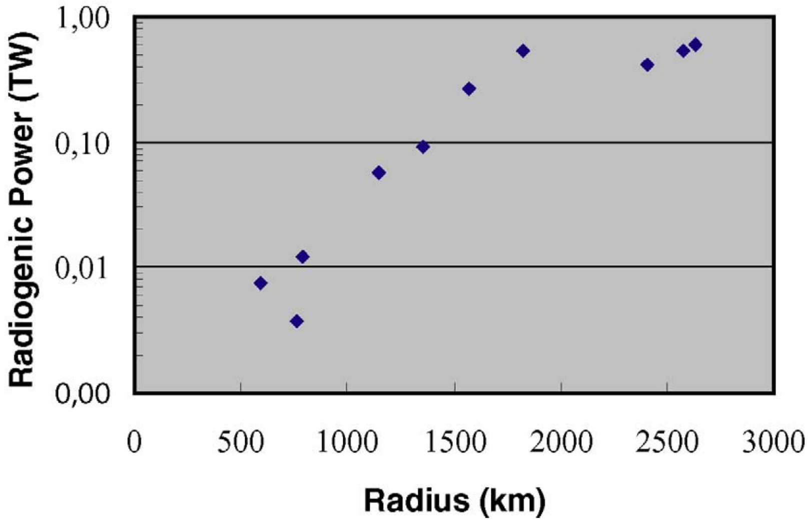


Fig. 1. Amount of internal radiogenic heating rate produced at present time within the largest icy satellites of the giant planets (24 TW for the Earth).

the EoS of each of those components must be known and laboratory experiments on ice have been important to develop realistic models of the icy satellite interior [19].

Gravity data were obtained during flybys of the Galilean satellites by the Galileo spacecraft. The gravity potential is determined by monitoring how the orbit of a spacecraft is modified by the mass of and the mass distribution within a planet. The degree zero of the spherical harmonic decomposition of gravity potential provides the mass ($M$) of the satellite:

$$M = \int_M \mathrm{d}m = 4\pi \int_0^R \rho(r) r^2 \,\mathrm{d}r \tag{1}$$

where radius $R$ is determined from limb images [20]. The mean density ($|\rho| = 3M/4\pi R^3$) can give a rough idea of the ice fraction. Assuming that the density of the non-ice fraction (silicates and iron core) is that of Io, an ice-free satellite, and that there is no other component than ice and silicates, one can estimate the silicate mass fraction and the amount of radiogenic power due to the decay of long-lived radiogenic isotopes (Table 1 and Fig. 1).

The degree 2 of the gravity potential can give access to the moment of inertia ($C$) [21–23]:

$$C = \int_M x^2 \,\mathrm{d}m = \frac{8\pi}{3} \int_0^R \rho(r) r^4 \,\mathrm{d}r \tag{2}$$

where $x$ is the distance of any elementary mass d$m$ to the rotation axis of the satellite. If the density does not vary with radius ($\rho(r) = const$), the MoI factor ($C/MR^2$) is equal to 0.4. The values for the Galilean satellites (Table 1) are smaller than 0.4, which implies that they are differentiated.

Although the joint inversion of mass and moment of inertia does not lead to a unique solution, it allows for bounding the thickness of each internal layer (Fig. 2). Thus, the thickness of the $H_2O$ layer on Europa has been roughly estimated at between 100 and 200 km [22,24]. For Ganymede and Callisto, the $H_2O$ layer would range between 600 and 900 km [23,24]. The large thickness of Ganymede and Callisto's $H_2O$ layer makes its structure quite different from that of Europa. Due to the high pressure value reached at the bottom of the $H_2O$ layer, high pressure ice phases must exist below a depth of roughly 150 km (Fig. 3). The $H_2O$ layer is subdivided in Ice Ih, Ice III, Ice V and Ice VI sublayers (Fig. 3). If a liquid layer exists, as suggested by the magnetic data [15,17,18], it should be located between the ice I and the ice V layer (e.g. [25], Figs. 2 and 3). In the case of Europa, the liquid layer should be directly in contact with the silicate interior. This particular configuration makes possible the chemical interaction between the water and the hotter silicate mantle, which has many exobiological implications [26].

The gravimetric data also show that the deep interior of Ganymede and Europa are probably differentiated into an iron-rich core and a silicate mantle [24,27]. Callisto, which has roughly the same size and density as Ganymede, is only partially differentiated [23,24,28]. Within the latter satellite, a mixed ice and rock layer with a density intermediate between ice and

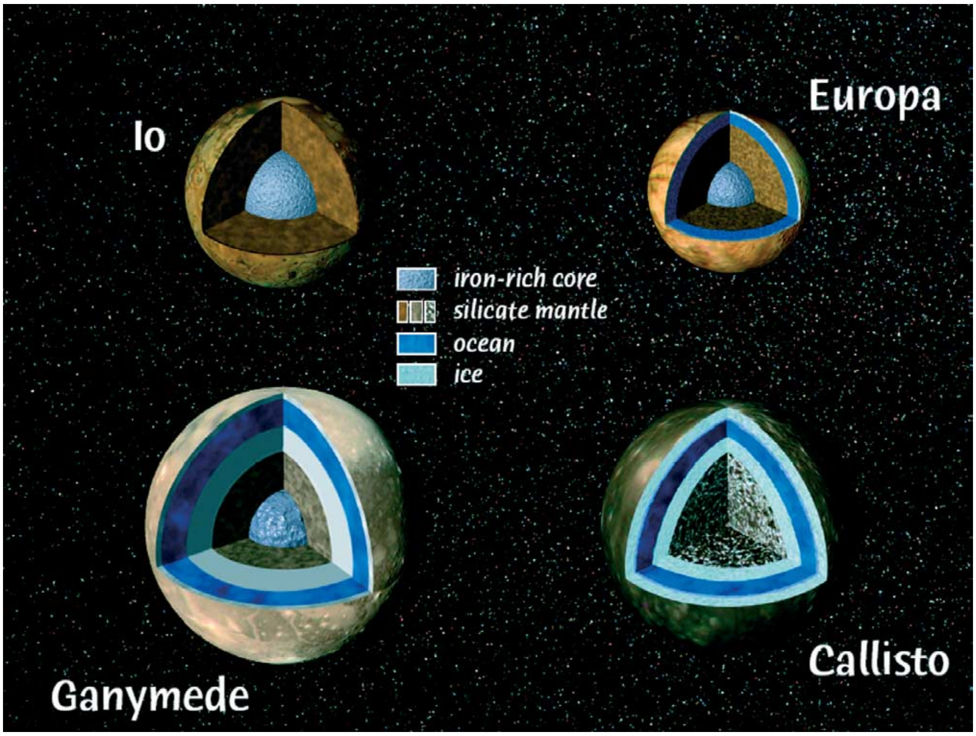


Fig. 2. Models of the internal structure of the Galilean satellites. The main difference between Europa and the two other icy satellites is that the liquid layer may be in contact with the silicate shell within Europa whereas a high-pressure ice shell should be present in between the liquid layer and the silicate shell within Ganymede and Callisto.

silicate, must still exist [24]. This suggests that the transfer of the radiogenic heat within Callisto has been sufficiently efficient to prevent the melting of ice and the subsequent segregation of the silicate-$H_2O$ mixture [28].

For Titan, no data are yet available to constrain its structure. Thermal evolution models [10,29] predict a differentiated structure similar to Ganymede [30]. This is suggested by the likely presence of ammonia in its interior, which reduces the melting temperature of ice [19]. However, the possibility of a partially differentiated structure similar to Callisto cannot be ruled out. Only the future measurements by the Cassini spacecraft [31] will provide very strong constraints on the present Titan interior and the possible evolution that it has undergone.

Analysis of the magnetic data shows that Europa, Ganymede and Callisto have an induced magnetic field as they orbit within Jupiter's magnetosphere [15,18]. One explanation is that these satellites have a conductive ocean under the icy crust [15,18]. It was discovered that Ganymede has a dipolar magnetic field in addition to the induced one. The few flybys allowed only for the determination of the degree 1 and 2 coefficients of the spherical harmonic decomposition of the magnetic field. By determining the lost of power between degree 1 and 2, the radius of a liquid iron core has been evaluated around 200 km [18].

The geophysical data give constraints on the present internal structure of the icy satellites. The next section describes models of the internal structure and thermal evolution models, which are compatible with these constraints.

## 3. Internal dynamics

Preliminary studies of the internal structure and thermal evolution of icy satellites were conducted prior to the Voyager mission in the late seventies (e.g. [32]). Subsolidus convection was not considered and the heat produced by the decay of radiogenic elements contained in a differentiated silicate core was supposed to be transferred by conduction. In an one-dimensional model, the surface heat flux ($q_S$) is proportional to the temperature gradient $(\mathrm{d}T/\mathrm{d}r)_{z=0}$:

$$q_S = \frac{Q}{4\pi R^2} = k\left(\frac{\partial T}{\partial r}\right)_{z=0} \tag{3}$$

where $Q$ is total power and $k$ is thermal conductivity. The thickness of the ice crust can be estimated very simply if one makes the following assumptions: (i) there is no heat production in the ice crust; (ii) thermal conductivity does not depend on

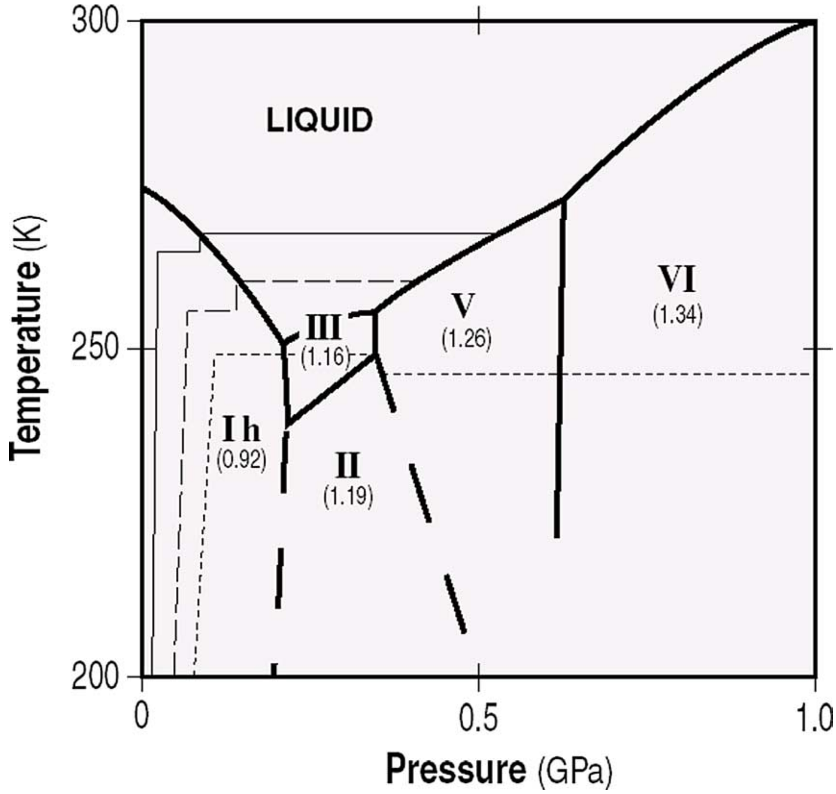


Fig. 3. Phase diagram of ice (with density). Three temperature profiles, corresponding to different stage of the satellite's evolution, are represented.

temperature; (iii) there is equilibrium between the radiogenic heating rate (Fig. 1) and the total heat power released; and (iv) the melting temperature is that of pure $H_2O$. For the largest icy satellites, these assumptions lead to a present heat flux around 8 $mW/m^2$, which provides a thickness of the order of 50 km. Subsequent studies [33,30,29] showed that the ice layer was unstable to convection for such large values.

### *3.1. Thermal convection*

Up to the mid-nineties, thermal convection models were calculated using isoviscous scaling laws [30]. Recent progresses in the modeling of thermal convection processes for fluids having complex viscosity have changed the scaling laws that one must apply in order to investigate the cooling rate of a planet [34–39]. Ignoring the possibility of tidal heating (Section 2.3), the ice crust can be modeled as a viscous fluid bounded by two isothermal boundaries: the surface ($T = 100$ K) and the ocean ($T = T_m$). In the case of a fluid with only temperature-dependent viscosity, numerical simulations [38] and laboratory experiments [40] suggest that the amount of heat that can be transferred by subsolidus convection is driven by the instabilities which form in the lower (hot) thermal boundary layer (TBL). Once stationary convection is reached, the thermal boundary layer is characterized by a constant value of the thermal boundary layer Rayleigh number ($Ra_{\mathrm{TBL}}$):

$$Ra_{\mathrm{TBL}} = \frac{\alpha \rho g (T_m - T_{\mathrm{ice}}) \delta^3}{\kappa \mu} \tag{4}$$

where $\delta$ is the thickness of the thermal boundary layer, $\alpha$ the coefficient of thermal expansion, $\mu$ the ice viscosity, $\kappa$ thermal diffusivity, and $T_{\mathrm{ice}}$ the temperature of the convective ice layer, which is the layer located between the two thermal boundary layers. The temperature difference ($T_m - T_{\mathrm{ice}}$) across the thermal boundary layer is proportional to a viscous temperature scale ($\Delta T_\mu$) [38]:

$$T_m - T_{\mathrm{ice}} = 1.43 \Delta T_\mu = 1.43 \left( \frac{-1}{(\partial Ln(\mu)/\partial T)_{T = T_{\mathrm{ice}}}} \right). \tag{5}$$

If one knows how ice viscosity depends on temperature, then one can calculate the temperature difference across the thermal boundary layer. Heat flux can be calculated using a law similar to Eq. (3):

$$q = \frac{Q}{4\pi R_m^2} = k\left(\frac{T_m - T_{\text{ice}}}{\delta}\right) \tag{6}$$

where $\delta$ is the TBL thickness determined by Eq. (4), and $R_m$ is the radius of the liquid-ice interface. Viscosity of ice is the key parameter controlling the amount of heat which can transferred by subsolidus convection (Section 4). Taking values of $10^{14}$ Pa.s for the viscosity of ice at its melting point and activation energies of 50 kJ/mol leads to a rapid freezing of the ocean in less than 1 Ga [38] for a simple model ignoring additional heat sources such as tidal dissipation, and presence of anti-freezing material such as ammonia. The next part describes the effect of tidal dissipation on heat transfer processes and the equilibrium state of $H_2O$ layer.

### *3.2. Tidal dissipation*

The large icy satellites of the giant planets are subjected to a periodical forcing (several days) as they travel around their respective giant planet, due to their orbital eccentricity (Table 1). Due to viscoelastic properties of their material, viscous dissipation occurs within their interior [41–44]. Tidal dissipation may represent a large internal energy source and it is invoked to explain the presence of an ocean within Europa [41,7,45–47]. This dissipation depends on the viscoelastic characteristics of each internal layer of the satellite [48], which are strongly temperature dependent.

Classically, the global tidal dissipation power in a planet is expressed as a function of the imaginary part of the Love number $k_2$:

$$Q_{\text{tide}} = -\frac{21}{2}\,\text{Im}(k_2)\frac{(\omega R^5)}{G}e^2 \tag{7}$$

where $w$ is the orbital angular frequency, $G$ is the universal gravitational constant, and $e$ the orbital eccentricity. The Love number $k_2$ describes the proportionality between the amplitude of the tide-rising potential and the induced potential. It is determined by integrating the equation of motion from the center to the surface of the satellite, so that the viscoelastic properties of each layer composing the satellite contributes the global $k_2$ value.

In the icy satellite interior with an internal ocean, most of dissipation occurs in the outer ice shell above the ocean. The decoupling effect induced by the ocean creates a high amplitude deformation of the ice shell, characterized by a maximum dissipation rate at the poles and a minimum on the equator at the sub-jovian and anti-jovian points [45,48]. Assuming a Maxwell rheology, the dissipation rate strongly depends on the value of the effective Newtonian viscosity at tidal strain rates. A peak value is found for viscosity values of $10^{14}$–$10^{15}$ Pa.s depending on the orbital eccentricity. The viscosity of the ice Ih layer is a major parameter to determine the global tidal dissipation rate within Europa, Ganymede, Callisto and Titan (Fig. 4). The

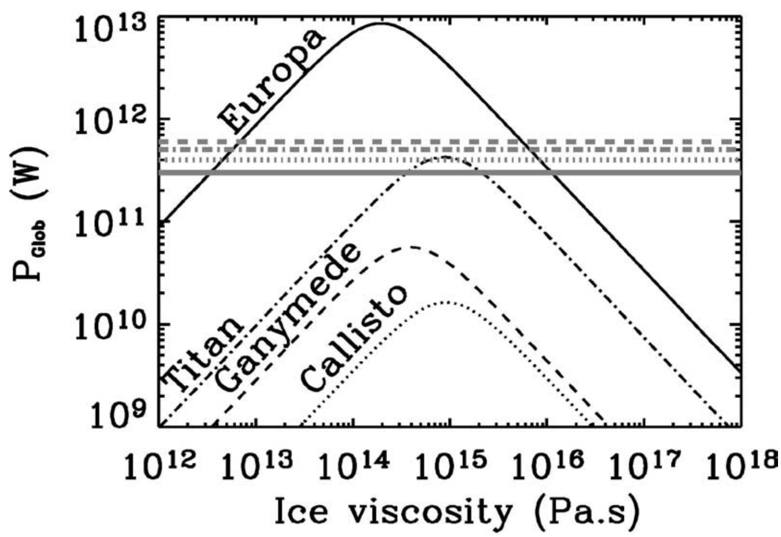


Fig. 4. Tidal heating in the Galilean icy satellites (after Tobie et al., [48]). Horizontal lines represent the present amount of radiogenic heating within the silicate core.

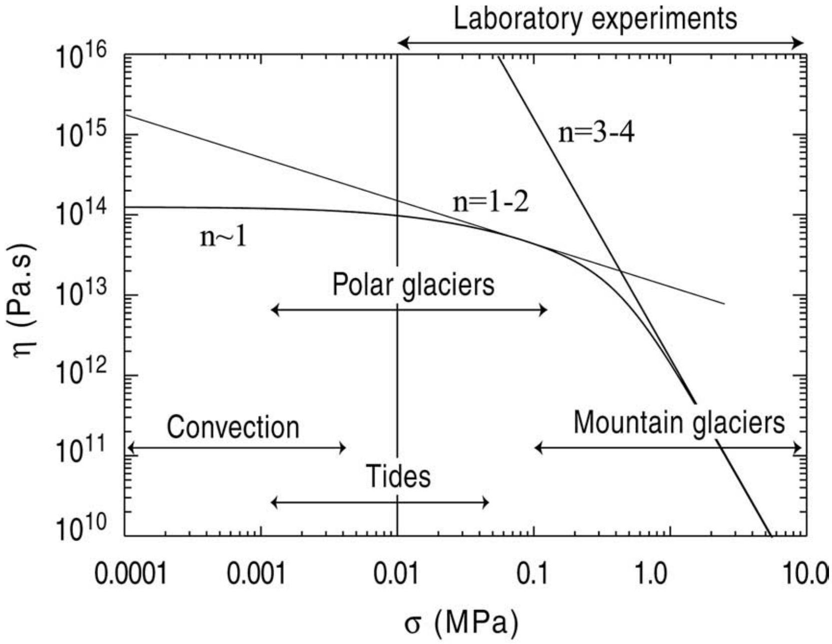


Fig. 5. Ice viscosity versus differential stress at constant temperature and grain size. The lower the differential stress, the smaller the stress exponent (Eq. (8)). This figure illustrates that the ice behaves as a Newtonian fluid at low differential stresses.

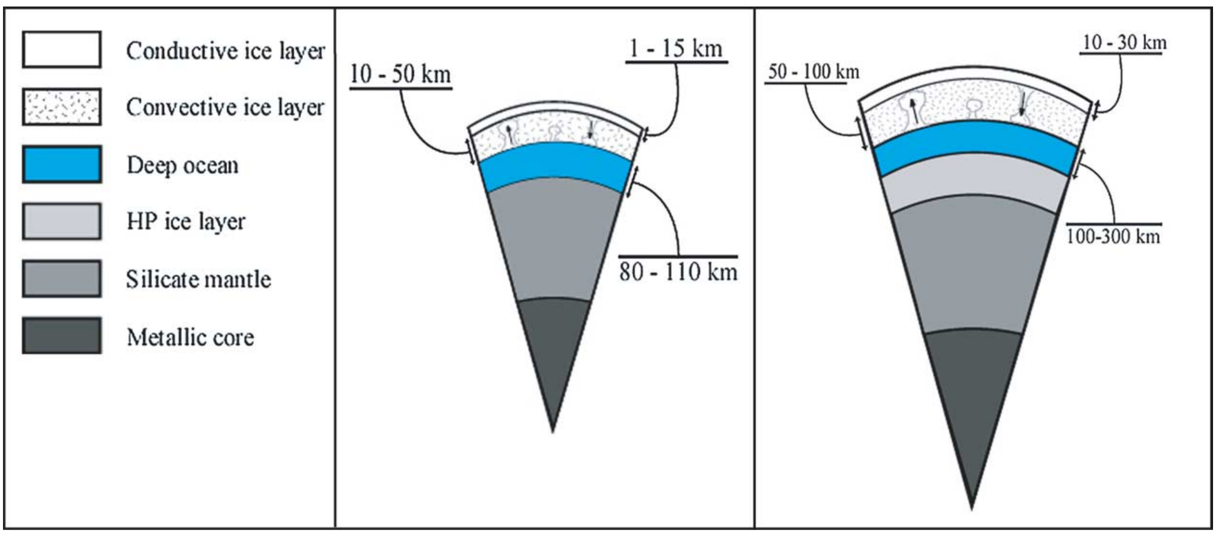


Fig. 6. Internal structure of large icy satellites. Europa (middle) may have an ocean in contact with the silicate shell. On the other hand, satellites with a large amount of ice, such as Ganymede, Callisto or Titan, (right), have a high-pressure ice layer in between the hypothetical ocean and the silicate core.

simulations described in Fig. 4 assume that there is an ocean below an ice Ih layer 50 km thick and a deep interior structure consistent with gravimetric data. Note that maximum dissipation occurs at viscosity values corresponding to the value that one can expect from the extrapolation of laboratory and Earth's ice sheet data for ice Ih near the melting point (Fig. 5).

In the case of Europa, the global dissipation generated in the outer ice shell is much larger than the radiogenic power provided by the silicate interior. Including tidal dissipation in thermal convection models modifies the geometry of convection and amount of heat which can be transferred through the ice crust [47]. Tidal dissipation within Europa's ice shell is so large than it can stabilize its thickness to a value of 20–25 km (Fig. 6). Tidal heating within Europa can also induce partial melting in convective hot plumes [49,47]. The presence of partial melt has several consequences. First, its strong effect on viscosity modifies the amount of tidal heating. Second, liquid is denser than Ice Ih and the density change produces a force in a direction opposite to that induced by thermal variations. This force may eventually overcome thermal buoyancy leading to hot plume collapse [47]. Third, as water forms at the expense of ice, the volume contraction in the upwelling plume may produce subsidence of the overlying outer rigid Ice Ih layer. This effect may explain the formation of chaotic terrains on Europa [49].

Although the current dissipation within Ganymede is low, one can expect large dissipation in the past when the satellite came into the Laplace resonance [50,44]. For Titan, the absence of significant resonance with any other Saturnian satellite implies a progressive decay of the eccentricity with time [43], suggesting that the eccentricity and consequently the tidal dissipation rate were higher in the past. A better knowledge of the ice mechanical properties is necessary, to describe accurately not only the thermal evolution of the icy satellites, but also their orbital evolution, which are coupled via tidal dissipation.

## 4. Physical and chemical properties of ice in icy satellite conditions

Models of the internal structure and dynamics of the icy satellites depend strongly on two parameters: the viscosity and phase diagram of ice. Viscosity controls the amount of tidal heating and the efficiency of heat transfer. The melting temperature is obviously a key parameter to explain the presence of liquid layers within some of these satellites. It is therefore necessary to understand how phase diagram depends on the impurities which may be present in addition to $H_2O$ ice. The following parts describe our current understanding on viscosity and phase diagram in icy satellite conditions.

### *4.1. Viscosity of ice Ih: extrapolation of laboratory and polar ice sheet data to icy satellite conditions*

Viscosity describes the ability of a material to deform continuously under a constant differential stress ($\tau$). It can be described as the ratio of the differential stress (or the second invariant of the stress tensor) to the strain rate ($\mathrm{d}\varepsilon/\mathrm{d}t$, where $\varepsilon$ is the deformation). Stress conditions typical of tidal deformation ($\tau_{\mathrm{tide}} = 0.01-0.1$ MPa) and convection ($\tau_{\mathrm{conv}} = 10^{-4}-10^{-3}$ MPa, [47]) cannot be reproduced by laboratory mechanical tests, so that an extrapolation of results from higher stresses is required. Rheological data for crystalline material are usually described with a power-law relationship:

$$\mathrm{d}\varepsilon/\mathrm{d}t = A\frac{\tau^n}{d^m}\exp\left(-\frac{Q+P\Delta V}{RT}\right) \quad \text{or} \quad \mu = \frac{1}{A}\tau^{1-n}d^m\exp\left(\frac{Q+P\Delta V}{RT}\right) \tag{8}$$

where $d$ is grain size, $m$ is grain size exponent, $n$ is the stress exponent, which varies according to the microscopic process responsible for creep (Fig. 5). At high stresses, the rheology of ice is governed by intra-crystalline dislocation slip mainly on basal planes with a stress exponent $n \sim 3$ [51,52]. At lower differential stresses ($\tau < 0.1$ MPa), the creep of ice may be controlled by Grain Boundary Sliding in case of very small grain sizes [53], or by both Dislocation Slip and Grain Boundary Sliding [54], or by Dislocation Slip accommodated by Grain Boundary Migration [55]. Several creep experiments also indicate a stress exponent lower than 2 for $\tau < 0.1$ MPa (see Table 4 in [53] for a review). The difficulty is to know how relevant are the extrapolation from experimental data to lower stresses ($< 0.01$ MPa), and how ice samples used in mechanical tests are characteristic of the icy crust of satellites such as Europa or Titan. Furthermore, numerous parameters may influence the creep of ice. At temperatures near the melting point ($T > 240$ K), normal grain growth and changes in the fabric significantly influence the creep mechanism. In addition, the cyclic straining experienced by ice on Europa over its 3.55 days orbital period may significantly modify its creep behavior. Thus, the rheological behavior of ice cannot be dissociated a priori from its strain history. However, since most of these aspects are strongly constrained by thermally activated processes, we can, at first attempt, assume that the effective viscosity of ice mainly depends on temperature. In addition, the creep data inferred from polar ice sheets [56] indicate that ice tends to behave like a Newtonian fluid ($n \sim 1$) at very low strain rates ($\frac{\mathrm{d}\varepsilon}{\mathrm{d}t} < 10^{-11}\ \mathrm{s}^{-1}$) and that the viscosity of ice near the melting point would be between $10^{13}$ and $10^{15}$ Pa.s.

### *4.2. Effect of partial melting*

Partial melting in upwelling 'hot' ice plumes is predicted in some numerical simulations for Europa [49,47]. The occurrence of partial melting is not due to adiabatic decompression of upwelling plumes as it is in the case of the partial melting of silicates in the Earth's mantle. It happens because the viscosity at melting temperature chosen in these simulations is that producing maximum tidal heating ($\mu = 1.5 \times 10^{14}$ Pa.s, Fig. 4). If one takes into account some uncertainty on the viscosity at melting temperature, the value could be as low as $10^{13}$ Pa.s or as large as $10^{15}$ Pa.s. Consequently, a value of $1.5 \times 10^{14}$ Pa.s is not in disagreement with our present knowledge of ice rheology. With this value, tidal heating is maximum in the hot plumes because temperature is larger in hot plumes than in cold plumes (Fig. 4). The melting rate is determined by the ratio of tidal heating to latent heat of melting.

As the partial melt is produced, the viscosity of ice decreases [57]. It has been suggested that 5% partial melt produces a viscosity decrease of about one order of magnitude [58]. Such an effect is taken into account in the present numerical simulations [47].

### 4.3. Viscosity of high-pressure ice

In the large icy satellites which contain more than 25% mass fraction of $H_2O$, the internal pressure is such that the presence of high pressure (HP) phases of ice is predicted. Depending upon the presence of a liquid layer, two mechanisms are envisaged to explain heat transfer through the HP ice. If a liquid layer is present, the equilibrium temperature profile lies along the melting curve of HP ice and heat is transferred by melting of ice at the silicate/HP ice interface and freezing of HP ice at the liquid layer/HP ice interface [50]. If there is no liquid layer, heat is transferred by subsolidus convection in the different ice layers [62, 30]. In the latter model, viscosity of HP ice controls the efficiency of convection. In both models, the viscosity of HP ice determines the amount of tidal heating.

There are few data available to constrain the viscosity of HP ice. Laboratory experiments have been carried out on ice V and ice VI using either a sapphire anvil cell [60,61] or Griggs-type apparatus [62,52]. As it has been discussed for Ice Ih (Fig. 5), the use of laboratory measurements is limited by our ability to extrapolate these results to conditions prevailing within icy satellites. As reported by previous studies [59,52], laboratory experiments have been carried out for differential stresses between 2 and 100 MPa whereas convective stresses are on the order of $10^{-3}$ MPa. However, the viscosity of ice VI seems to be low enough for convection processes to operate in the ice VI layer in a model where there is no ocean.

### 4.4. Phase diagram

The phase diagram of pure $H_2O$ (Fig. 3) has been investigated for a long time [63] and the liquidus of pure $H_2O$ is well known in the pressure range of interest for the icy satellites ($P < 2$ GPa). However, other compounds such as methane or/and ammonia may have been present during the formation of these satellites [64,4]. Ammonia is important because it is well known to be very effective in lowering the melting temperature of ice. At room pressure, the melting temperature of a mixture of water and ammonia is about 100 K lower than that of pure $H_2O$ [65]. Methane exists in Titan's atmosphere and must be another important compound of ice. Finally, alteration of silicates during accretion and subsequent differentiation may have produced different compounds such as sulfates. One can note that magnesium sulfates such as epsomite are one candidate to explain the non-ice infrared absorption observed by NIMS/Galileo [66].

Laboratory experiments have been carried out to investigate the phase diagram of $H_2O$-$NH_3$ at pressures relevant to the interior of icy satellites [67–70]. The main result is the following: as the icy satellite cools, $H_2O$ ice freezes both on top of the ocean (Ice Ih) and at the bottom (ice V). The ocean gets more and more enriched in ammonia and its temperature may eventually get much lower than the melting temperature of $H_2O$ ice. Because the viscosity of the outer Ice Ih layer becomes larger, the amount of heat that can be transferred by convection decreases and an equilibrium is reached [71,38]. The presence of ammonia maintains a liquid layer in between the outer Ice Ih layer and the inner HP ice layers.

Methane is a minor component of Titan's atmosphere but an understanding of its cycle puts constraints on the dynamics and structure of Saturn's largest satellite. A source of methane is required in order to explain its presence in Titan's atmosphere since it transforms irreversibly into ethane by photo-dissociation [72]. Several possibilities have been envisaged, including methane oceans at the surface [73], subsurface reservoirs [72], or cryovolcanism [10]. Recent laboratory experiments on the stability of methane clathrate at high-pressure [74] suggest that low pressure methane clathrate transforms into a stable high-pressure phase at 1 GPa and remains stable up to at least 10 GPa. With such constrains, it becomes difficult to understand the destabilization of methane and its migration to the surface. However, little is known for the system $H_2O$-$NH_3$-$CH_4$. Because theoretical models based on the calculation of free Gibbs energy for the different phases [75] have proven to not be verified by laboratory experiments even for the simple $H_2O$-$NH_3$ system or $H_2O$-$CH_4$ system, laboratory experiments in the pressure range of interest for the interior of Titan are required in order to understand and to model the methane cycle within Titan.

## 5. Concluding remarks

The large icy satellites of Jupiter are fascinating objects which have been observed by the Galileo mission. Understanding the different sets of observation (gravity and magnetic field, surface tectonics and composition) requires models of their internal structure and dynamics which include laboratory data on the physical and chemical properties of ice. Theoretical studies that have been carried out since the late seventies show the importance of heat transfer by thermal convection, of anti-freezing component such as ammonia, and of heat generation by tidal friction, in the modeling of interior evolution. New experimental data on ice properties in a wide range of temperature and pressure are required to constrain these different aspects and improve the quality of the models.

The next step in the exploration of this family of planetary objects will be provided by the Cassini–Huygens mission which will start orbiting Saturn in July 2004. The numerous flybys of Titan, its largest satellite, will provide us with some new observations on this class of objects. There is a strong need for laboratory experiments in order for the models to include laboratory data on the physical and chemical properties of clathrate hydrates. In a 'far' future, a mission to Europa is envisaged (JIMO) in order to demonstrate the existence of an ocean and to test the possibility of volcanism at the ocean-silicate interface.

## Acknowledgements

This study was supported by INSU/CNES Programme National de Planétologie and Programme Lavoisier du Ministère des Affaires Etrangères. We thank Olivier Grasser, Antoine Mocquet and Paul Duval for very fruitful discussions.

## References

[1] D. Gautier, T. Owen, The composition of outer planet atmospheres, in: S.K. Atreya, J.B. Pollack, M.S. Matthews (Eds.), Origin and Evolution of Planetary and Satellite Atmospheres (A89-43776 19-90), University of Arizona Press, Tucson, AZ, 1989, pp. 487–512.
[2] W.B. Hubbard, Structure and composition of giant planet interiors, in: S.K. Atreya, J.B. Pollack, M.S. Matthews (Eds.), Origin and Evolution of Planetary and Satellite Atmospheres (A89-43776 19-90), University of Arizona Press, Tucson, AZ, 1989, pp. 539–563.
[3] I. Mosqueira, P.R. Estrada, Formation of the regular satellites of giant planets in an extended gaseous nebula I: subnebula model and accretion of satellites, Icarus 163 (2003) 198–203.
[4] O. Mousis, D. Gautier, D. Bockelée-Morvan, An evolutionary turbulent model of Saturn's subnebula: Implications for the origin of the atmosphere of Titan, Icarus 156 (2002) 162–175.
[5] D.L. Matson, G.A. Ransford, T.V. Johnson, Heat flow from Io(JI), J. Geophys. Res. 86 (1981) 1664–1672.
[6] R.T. Pappalardo, et al., Geologic evidence for solid-state convection in Europa's ice shell, Nature 391 (1998) 365–368.
[7] S.W. Squyres, R.T. Reynolds, P. Cassen, Liquid water and resurfacing on Europa, Nature 301 (1983) 225–226.
[8] S.K. Croft, Mimas: Tectonic structure and geologic history, NASA, Washington, Reports of Planetary Geology and Geophysics Program (1990) 95–97.
[9] J.S. Kargel, S. Pozio, The volcanic and tectonic history of Enceladus, Icarus 119 (1996) 385–404.
[10] J. Lunine, D.J. Stevenson, Clahtrates and ammonia hydrates at high pressure: application to the origin of methane on Titan, Icarus 70 (1987) 61–77.
[11] L.A. Soderblom, T.L. Becker, S.W. Kieffer, R.H. Brown, C.J. Hansen, T.V. Johnson, Triton's geyser-like plumes – Discovery and basic characterization, Science 250 (1990) 410–415.
[12] J.I. Lunine, S.K. Atreya, J.B. Pollack, Present state and chemical evolution of the atmospheres of Titan, Triton and Pluto, in: S.K. Atreya, J.B. Pollack, M.S. Matthews (Eds.), Origin and Evolution of Planetary and Satellite Atmospheres (A89-43776 19-90), University of Arizona Press, Tucson, AZ, 1989, pp. 605–665.
[13] A. Coradini, P. Cerroni, G. Magni, C. Federico, Formation of the satellites of the outer solar system, in: S.K. Atreya, J.B. Pollack, M.S. Matthews (Eds.), Sources of their Atmospheres in Origin and Evolution of Planetary and Satellite Atmospheres (A89-43776 19-90), University of Arizona Press, Tucson, AZ, 1989, pp. 723–762.
[14] M.H. Carr, et al., Evidence for a subsurface ocean on Europa, Nature 391 (1998) 363–365.
[15] K.K. Khurana, M.G. Kivelson, C.T. Russell, Induced magnetic fields as evidence for subsurface ocean in Europa and Callisto, Nature 397 (1998) 777–780.
[16] R.T. Pappalardo, et al., Does Europa have a subsurface ocean? Evaluation of the geological evidence, J. Geophys. Res. 104 (1999) 24015–24056.
[17] M.G. Kivelson, K.K. Khurana, K. Krishan, C.T. Russell, M. Volwerk, R.J. Walker, C. Zimmer, Galileo magnetometer measurements: A stronger case for a subsurface ocean at Europa, Science 289 (2000) 1340–1343.
[18] M.G. Kivelson, K.K. Khurana, M. Volwerk, The permanent and inductive magnetic moments of Ganymede, Icarus 157 (2002) 507–522.
[19] C. Sotin, O. Grasset, S. Beauchesne, Thermodynamic properties of high pressure ices: Implications for the dynamics and internal structure of large icy satellites, in: B. Schmitt, et al. (Eds.), Solar System Ices, 1998, pp. 79–96.
[20] P.C. Thomas, M.E. Davies, T.R. Colvin, J. Oberst, P. Schuster, G. Neukum, M.H. Carr, A. McEwen, G. Schubert, M.S.J. Belton, The shape of Io from Galileo limb measurements, Icarus 135 (1998) 175–180.
[21] J.D. Anderson, E.L. Lau, W.L. Sjogren, G. Schubert, W.B. Moore, Gravitational constraints on the internal structure of Ganymede, Nature 384 (1996) 541–543.
[22] J.D. Anderson, G. Schubert, R.A. Jacobson, E.L. Lau, W.B. Moore, W.L. Sjogren, Europa's differentiated internal structure: inferences from four Galileo encounters, Science 281 (1998) 2019–2022.
[23] J.D. Anderson, R.A. Jacobson, T.P. McElrath, W.B. Moore, G. Schubert, P.C. Thomas, Shape, mean radius, gravity field, and the interior structure of Callisto, Icarus 153 (2001) 157–161.

[24] F. Sohl, T. Spohn, D. Breuer, K. Nagel, Implications from Galileo observations on the interior structure and chemistry of the Galilean satellites, Icarus 157 (2002) 104–119.
[25] T. Spohn, G. Schubert, Oceans in the icy Galilean satellites of Jupiter? Icarus 161 (2003) 456–467.
[26] J.S. Kargel, J.Z. Kaye, J.W. Head, G.M. Marion, R. Sassen, J.K. Crowley, O.P. Ballesteros, S.A. Grant, D.L. Hogenboom, Europa's crust and ocean: Origin, composition, and the prospects for life, Icarus 148 (2000) 226–265.
[27] D.J. Stevenson, When Galileo met Ganymede, Nature 384 (1996) 511–512.
[28] K. Nagel, D. Breuer, T. Spohn, A model for the interior structure, evolution and differentiation of Callisto, Icarus 169 (2004) 402–412.
[29] O. Grasset, C. Sotin, F. Deschamps, On the internal structure and dynamics of Titan, Planet. Space Sci. 48 (2000) 617–636.
[30] R.L. Kirk, D.J. Stevenson, Thermal evolution of a differentiated Ganymede and implications for surface features, Icarus 69 (1987) 91–134.
[31] N. Rappaport, B. Bertotti, G. Giampieri, J.D. Anderson, Doppler measurements of the quadrupole moments of Titan, Icarus 126 (1997) 313–323.
[32] G.J. Consolmagno, J.S. Lewis, The evolution of icy satellite interiors and surfaces, Icarus 34 (1978) 280–293.
[33] G. Schubert, D.J. Stevenson, K. Ellsworth, Internal structures of the Galilean satellites, Icarus 47 (1981) 46–59.
[34] A. Davaille, C. Jaupart, Transient high-Rayleigh number thermal convection with large viscosity variations, J. Fluid Mech. 253 (1993) 141–166.
[35] L.N. Moresi, V.S. Solomatov, Numerical investigation of 2D convection with extremely large viscosity variations, Phys. Fluids 7 (1995) 2154–2162.
[36] O. Grasset, E.M. Parmentier, Thermal convection in a volumetrically heated, infinite Prandtl number fluid with strongly temperature-dependent viscosity: implications for planetary thermal evolution, J. Geophys. Res. 103 (1998) 18171–18181.
[37] C. Dumoulin, M.-P. Douin, L. Fleitout, Heat transport in stagnant lid convection with temperature and pressure dependent Newtonian and non-Newtonian rheology, J. Geophys. Res. 104 (1999) 12759–12778.
[38] F. Deschamps, C. Sotin, Thermal convection in the outer shell of large icy, J. Geophys. Res. 106 (2001) 5107–5122.
[39] C.C. Reese, V.S. Solomatov, L.-N. Moresi, Non-Newtonian stagnant lid convection and magmatic resurfacing on Venus, Icarus 139 (1999) 67–80.
[40] M. Manga, D. Weeraratne, Experimental study of a non-Boussinesq Rayleigh–Bénard convection at high Rayleigh and Prandtl numbers, Phys. Fluid 11 (1999) 2969–2976.
[41] P. Cassen, R.T. Reynolds, S.J. Peale, Is there liquid water on Europa, Geophys. Res. Lett. 6 (1979) 731–734.
[42] J.-P. Poirier, L. Boloh, P. Chambon, Tidal dissipation in small viscoelastic ice moons: the case of Enceladus, Icarus 55 (1983) 218–230.
[43] F. Sohl, W.D. Sears, R.D. Lorenz, Tidal dissipation on Titan, Icarus 115 (1995) 278–294.
[44] A.P. Showman, R. Malhotra, Tidal evolution into the Laplace resonance and the resurfacing of Ganymede, Icarus 127 (1997) 93–111.
[45] G.W. Ojakangas, D.J. Stevenson, Thermal state of an ice shell on Europa, Icarus 81 (1989) 220–241.
[46] H. Hussmann, T. Spohn, K. Wieczerkowski, Thermal equilibrium states of Europa's ice shell: Implications for internal ocean thickness and surface heat flow, Icarus 156 (2002) 143–151.
[47] G. Tobie, G. Choblet, C. Sotin, Tidally heated convection: Constraints on Europa's ice shell thickness, J. Geophys. Res. 108 (E11) (2003), CiteID 5124.
[48] G. Tobie, A. Mocquet, C. Sotin, Tidal dissipation within large icy satellites: Europa and Titan, Icarus (2004), in press.
[49] C. Sotin, J. Head, G. Tobie, Europa: Tidal heating of upwelling thermal plumes and the origin of lenticulae and chaos melting, Geophys. Res. Lett. 29 (2002) 74-1–74-4.
[50] P. Cassen, S.J. Peale, R.T. Reynolds, On the comparative evolution of Ganymede and Callisto, Icarus 41 (1980) 232–239.
[51] W.F. Budd, T.H. Jacka, A review of ice rheology for ice sheet modelling, Cold Reg. Sci. Technol. 16 (1989) 107–144.
[52] W.B. Durham, S.H. Kirby, L.A. Stern, Creep of water ices at planetary conditions: A compilation, J. Geophys. Res. 102 (1997) 16293–16302.
[53] D.L. Goldsby, D.L. Kohlstedt, Superplastic deformation of ice: Experimental observations, J. Geophys. Res. 106 (2001) 11017–11030.
[54] W.B. Durham, L.A. Stern, S.H. Kirby, Rheology of ice I at low stress and elevated confining pressure, J. Geophys. Res. 106 (2001) 11031–11042.
[55] P. Duval, M. Montagnat, Comment on "Superplastic deformation of ice: Experimental observations", by D.L. Goldsby and D.L. Kohlstedt, J. Geophys. Res. 107 (B4) (2002), CiteID 2082.
[56] M. Montagnat, P. Duval, Rate controlling processes in the creep of polar ice, influence of grain boundary migration associated with recrystallization, Earth Planet. Sci. Lett. 183 (2000) 179–186.
[57] P. Duval, The role of the water content on the creep rate of polycrystalline ice, in: Isotopes and Impurities in Snow and Ice, in: IAHS Publ., vol. 118, 1977, pp. 29–33.
[58] S. De La Chapelle, H. Milsch, O. Castelnau, P. Duval, Compressive creep of ice containing a liquid intergranular phase: rate-controlling processes in the dislocation creep regime, Geophys. Res. Lett. 26 (1999) 251–254.
[59] C. Sotin, Viscosité des glaces et dynamique de Ganymède, B. Soc. Géol. Fr. 1 (1987) 107–112.
[60] J.-P. Poirier, C. Sotin, J. Peyronneau, Viscosity of high-pressure ice VI and dynamics of Ganymede, Nature 292 (1981) 225–227.
[61] C. Sotin, J.-P. Poirier, The sapphire anvil cell as a creep apparatus, in: Duba, et al. (Eds.), The Brittle-Ductile Transition in Rocks: The Heard Volume, in: Geophysical Monograph, vol. 56, AGU, 1990, pp. 219–223.
[62] W.B. Durham, L.A. Stern, S.H. Kirby, Rheology of water ices V and VI, J. Geophys. Res. 101 (1996) 2989–3002.
[63] P.W. Bridgman, Water in the liquid and five solid forms under pressure, P. Am. Acad. Arts Sci. 47 (1911) 441.
[64] R.G. Prinn, B. Fegley, Kinetic inhibition of CO and $N_2$ reduction in circumplanetary nebulae – Implications for satellite composition, Astrophys. J. 249 (1981) 308–317.
[65] A.P. Rollet, G. Vuillard, Sur un nouvel hydrate de l'ammoniac, C. R. Acad. Sci. Paris 243 (1956) 383–386.

[66] T. McCord, et al., Non-water-ice constituents in the surface material of the icy Galilean satellites from the Galileo near-infrared mapping spectrometer investigation, J. Geophys. Res. 103 (1998) 8603–8626.
[67] S. Boone, M.F. Nicol, Ammonia-water mixtures at high pressures – Melting curves of ammonia dihydrate and ammonia monohydrate and a revised high-pressure phase diagram for the water-rich region, in: Lunar and Planetary Science Conference, 21st, Houston, TX, Proceedings A91-42332 17-91, 1991, pp. 603–610.
[68] O. Grasset, S. Beauchesne, C. Sotin, Etude par spectrométrie Raman in situ du diagramme de phase de $NH_3$-$H_2O$ dans le domaine 10 MPa–1.5 GPa : application à la dynamique de Titan, C. R. Acad. Sci. Paris, Ser. IIa 320 (1995) 249–256.
[69] D.L. Hogenboom, J.S. Kargel, G.J. Consolmagno, T.C. Holden, L. Lee, M. Buyyounouski, The ammonia–water system and the chemical differentiation of icy satellites, Icarus 128 (1997) 171–180.
[70] O. Mousis, J. Pargamin, O. Grasset, C. Sotin, Experiments in the $NH_3$-$H_2O$ system in the $[0, 1\text{ GPa}]$ pressure range – implications for the deep liquid layer of large icy satellites, Geophys. Res. Lett. 29 (2002), CiteID 2192.
[71] O. Grasset, C. Sotin, The cooling rate of a liquid shell in Titan's interior, Icarus 123 (1996) 101–112.
[72] J. Lunine, Does Titan have oceans, Am. Sci. 82 (1994) 134–143.
[73] D.B. Campbell, G.J. Black, L.M. Carter, S.J. Ostro, Radar evidences for liquid surfaces on Titan, Science 300 (2003) 431–434.
[74] J.S. Loveday, R.J. Nelmes, M. Guthrie, S.A. Belmonte, D.R. Allan, D.D. Klug, J.S. Tse, Y.P. Handa, Stable methane hydrate above 2 GPa and the source of Titan's atmospheric methane, Nature 410 (2001) 661–663.
[75] J. Lunine, D.J. Stevenson, Thermodynamics of clathrate hydrate at low and high pressures with application to the outer solar system, Astrophys. J. Suppl. Series 58 (1985) 493–531.